Proceedings of the Ninth Pacific Conference on Earthquake Engineering
Building an Earthquake-Resilient Society
14-16 April, 2011, Auckland, New Zealand

A simple approach to real-time fault detection and diagnosis in base-isolation systems

Mostafa Nayyerloo[1,3] & Leonardo Acho

[1]*CoDAlab, Departament de Matemàtica Aplicada III, Escola Universitària d'Enginyeria Tècnica Industrial de Barcelona, Universitat Politècnica de Catalunya, Comte d'Urgell, 187, 08036 Barcelona, Spain*

José Rodellar

[2]*CoDAlab, Departament de Matemàtica Aplicada III, Escola Tècnica Superior d'Enginyers de Camins, Canals i Ports de Barcelona, Universitat Politècnica de Catalunya, Jordi Girona, 1–3, 08034 Barcelona, Spain*

J. Geoffrey Chase & XiaoQi Chen

[3]*Department of Mechanical Engineering, University of Canterbury, Private Bag 4800, Christchurch 8140, New Zealand*

ABSTRACT: In recent years, base-isolation has become an increasingly applied structural design technique in highly seismic areas. The state-of-the-art practice is to use active or passive magneto-rheological (MR) dampers to limit the base displacement. The crucial effect of likely faults in the base-isolation system on the top superstructure requires that the resulting nonlinear hysteretic system to be monitored in real-time for possible changes in the two most important structural parameters: stiffness and damping.

This paper develops a simple fault detection and diagnosis technique based on comparing the internal dynamics of the base-isolation system with those of a healthy baseline model to detect faults. Three different cases of stiffness, damping, and combined stiffness and damping faults are studied, *in silico*, on a realistic base-isolated structure subjected to the Loma Prieta earthquake with a passive MR damper. The simulation results show that the proposed fault detection and diagnosis algorithm is well capable of detecting the existence, determining the type, and quantifying the severity of faults in the system in real-time as the faults occur.

1 INTRODUCTION

Base-isolation systems decouple structures from the ground to protect the integrity of structures against seismic excitations. The current practice is to use passive, semi-active, or active dampers such as magneto-rheological (MR) dampers at the base level to seismically isolate the structure from the shaking ground (Spencer and Nagarajaiah 2003). The performance of the resulting nonlinear hysteretic system at the isolation level directly affects the seismic behaviour of its top superstructure. Therefore, the base-isolation system needs to be monitored for likely faults to reliably maintain the superstructure's integrity.

In nonlinear control theory, fault detection and diagnosis have attracted significant attention, particularly for highly sensitive systems where fault detection at the earliest stage is required (Patton 1997; Duan and Patton 1998; Edwards et al. 2000; Saif 2002; Liberatore et al. 2006; Mhaskar et al. 2008). The process of fault detection and diagnosis is often referred to as structural health monitoring (SHM) in the mechanical, aerospace, and the civil engineering fields. Fault detection is typically done by means of a residual signal generated from available measurements (Besançon 2003). It must be a

signal which is zero or near zero in the absence of faults and considerably affected when the system is undergoing faults (Kinnaert 1999; Besançon 2003; Liberatore et al. 2006). In addition, the residual signal has to return to its original no-fault state when the faults fade away.

Different fault detection and diagnosis algorithms have been proposed in the literature such as (Duan and Patton 1998; Edwards et al. 2000; Saif 2002), but they all come with significant complexity. This paper develops a simple fault detection technique based on a comparison between the internal dynamics of the base-isolation system with a healthy baseline model's internal dynamics to detect likely faults. The residual signal is then used for fault quantification using least squares fitting techniques. Different combinations of stiffness and damping faults are considered for proof-of-concept simulations on a passive second-order base-isolated system. The choice of passive system is only for simplicity, and it is straightforward to generalize the method developed to active and semi-active base-isolation systems.

2 SHM PROBLEM STATEMENT

A nonlinear seismically excited base-isolation system with passive MR dampers can be modelled:

$$m\ddot{v}(t) + c\dot{v}(t) + \alpha k v(t) + (1-\alpha)kYz(t) = -m\ddot{x}_g(t) \tag{1}$$

where m, c, and k are the mass, damping, and the stiffness of the system, respectively, v, $\dot{v}$, and $\ddot{v}$ are displacement, velocity, and acceleration of the base-isolation system, respectively, $0 < \alpha < 1$ is the bi-linear factor defined as the post to pre-yield stiffness ratio of the system, and $\ddot{x}_g$ is the ground motion acceleration. Moreover, $z(t)$ is the dimensionless Bouc-Wen hysteresis component governed by the following first-order differential equation from the so-called classical Bouc-Wen model (Bouc 1967; Wen 1976; Constantinou and Tadjbakhsh 1985; Ismail et al. 2009):

$$\dot{z}(t) = \frac{A\dot{v}(t) - \beta\left|\dot{v}(t)\right|\left|z(t)\right|^{n-1} z(t) - \gamma\dot{v}(t)\left|z(t)\right|^{n}}{Y} \tag{2}$$
$$A > 0, \beta > 0, -\beta \le \gamma \le \beta, n > 0$$

where A, β, γ, and n are stiffness, loop fatness, loop pinching, and abruptness parameters in the classical Bouc-Wen model, respectively. Further, n, the power factor, determines the sharpness of the curve from elastic to plastic force-deflection behaviour of the system, and finally, Y is the yield displacement of the system.

When a fault occurs in a base-isolation system, assuming the mass and the internal parameters of the damper remain unchanged, the equations of motion of the faulty or damaged system can be written:

$$m\ddot{\bar{v}}(t) + \left(c + \Delta c(t)\right)\dot{\bar{v}}(t) + \alpha\left(k + \Delta k(t)\right)\bar{v}(t) + (1-\alpha)\left(k + \Delta k(t)\right)Y\bar{z}(t) = -m\ddot{x}_g(t) \tag{3}$$

where $\ddot{\bar{v}}$, $\dot{\bar{v}}$, and $\bar{v}$ are responses of the faulty system, and Δk and Δc respectively denote time-varying changes in the stiffness and damping of the system due to the fault. Further, $\bar{z}(t)$ is the hysteretic component of the faulty structure from Equation (2) using velocities of the faulty base-isolation system. The problem is to design a fault or damage detection signal that is zero in the absence of fault and non-zero with amplitude relative to the severity of the fault when it occurs. Such signals are called residual signals in fault detection systems. In addition to fault detection, the designed residual signal should provide enough information for diagnosis of the fault detected, such as enabling the identification of time-varying Δk and Δc terms in Equation (3).

3 RESIDUAL SIGNAL DESIGN

The Bouc-Wen model used to represent the internal dynamics of base-isolation systems has only one state variable. Therefore, any change in the dynamic behaviour of the system will appear in this single

state. This suggests rearranging Equation (3) in the form of Equation (4) by introducing a new hysteretic component, $\overline{Z}(t)$, for the faulty or damaged system:

$$m\ddot{\overline{v}}(t)+c\dot{\overline{v}}(t)+\alpha k\overline{v}(t)+(1-\alpha)kY\overline{Z}(t)=-m\ddot{x}_g(t) \tag{4}$$

where

$$\overline{Z}(t)=\left(1+\frac{\Delta k(t)}{k}\right)\overline{z}(t)+\frac{\alpha\Delta k(t)}{(1-\alpha)kY}\overline{v}(t)+\frac{\Delta c(t)}{(1-\alpha)kY}\dot{\overline{v}}(t) \tag{5}.$$

A simple comparison between Equations (1) and (4) shows that these two equations are essentially the same except in the hysteretic components. Therefore, comparing the internal dynamics of the two healthy and faulty systems by taking the difference between the hysteretic components reveals any likely changes (faults) in the system. As Equation (5) shows, in the absence of a fault, where $\Delta k=\Delta c=0$, $\overline{Z}(t)=\overline{z}(t)$ and thus $\overline{Z}(t)-\overline{z}(t)$ is zero. When there is a fault in the system, $\overline{Z}(t)\neq\overline{z}(t)$ and the residual, $\overline{Z}(t)-\overline{z}(t)$, is non-zero. Hence, this difference can be used as an indication for the existence of stiffness or damping faults in the base-isolation system:

$$I(t)=\kappa_1\left(\overline{Z}(t)-\overline{z}(t)\right) \tag{6}$$

where $I(t)$ is the residual signal and $\kappa_1>0$ is a scaling factor.

The same changes in the stiffness and damping of the system typically do not result in the same residual signals. Changes in the damping coefficient usually have much less effect on the structural responses and consequently on the designed residual signal. This difference in the effect of the two different types of fault with same severity on the base-isolation system makes presentation of results for combined cases of fault difficult. Therefore, two more scaling factors, $\kappa_2,\kappa_3>0$, are introduced to overcome this problem:

$$I(t)=\frac{\kappa_1}{kY}\left[\kappa_2\Delta k(t)\left(Y\overline{z}(t)+\frac{\alpha}{1-\alpha}\overline{v}(t)\right)+\frac{\kappa_3\Delta c(t)}{(1-\alpha)}\dot{\overline{v}}(t)\right] \tag{7}$$

where again $I(t)$ is the residual signal, and all other terms have been previously defined. To calculate the residual signal in Equation (6), $\overline{Z}$ is calculated from Equation (4) using measured responses of the faulty system and measured ground accelerations. The internal dynamics of the healthy system, $\overline{z}$, is estimated by calculating its first time derivative, $\dot{\overline{z}}$, from Equation (2) using measured velocities of the faulty structure and assuming zero initial state. All other terms in Equations (2) and (4), including the Bouc-Wen and structural parameters, are either measured or assumed to be known prior to fault detection to present the healthy dynamics of the base-isolation system in the absence of damaging inputs.

4 FAULT DIAGNOSIS

The aim of the diagnostic part is to determine the type and severity of likely faults detected by the residual signal in the base-isolation system. Quantifying detected faults, for instance in terms of initial stiffness and/or damping values of the system, is of great importance in structural health monitoring and provides required information by structural control methods with damage control or mitigation purposes. Detected faults could be of stiffness type ($\Delta k\neq 0$), damping type ($\Delta c\neq 0$), or a combination of both ($\Delta k,\ \Delta c\neq 0$). Therefore, identifying Δk and Δc in Equation (7) determines the fault type, as well as its severity. To identify Δk and Δc in real-time, Equation (7) can be rewritten at each time step Δt_k:

$$I_k = \phi_{1,k}\Delta k_k + \phi_{2,k}\Delta c_k \tag{8}$$

where

$$\begin{aligned}\phi_{1,k} &= \frac{\kappa_1\kappa_2}{kY}\left(Y\overline{z}_k + \frac{\alpha}{1-\alpha}\overline{v}_k\right)\\ \phi_{2,k} &= \frac{\kappa_1\kappa_3}{kY(1-\alpha)}\dot{\overline{v}}_k\end{aligned} \tag{9}$$

and subscript k denotes values at time k. In Equation (9), $\dot{\overline{v}}_k$ and $\overline{v}_k$, responses of the faulty system at each time step are measured, $\overline{z}_k$ is estimated from Equation (2) using measured velocities of the faulty system, κ_{1-3} are user selected tuning factors, and all other parameters are assumed to be *a priori* known. These parameters are mainly design parameters of the base-isolation system and are typically available before fault detection and diagnosis. Thus, $\phi_{1,k}$ and $\phi_{2,k}$ can be readily calculated at each time step. Moreover, as it was mentioned earlier, $\overline{Z}_k$ is calculated from Equation (4) using measured responses of the faulty system, measured ground motion acceleration, and known parameters of the healthy system. Therefore, from Equation (6), I_k is known, and Equation (8) is a linear equation in terms of the unknowns (Δk_k and Δc_k) at each time step Δt_k and can be solved using piecewise least squares estimation.

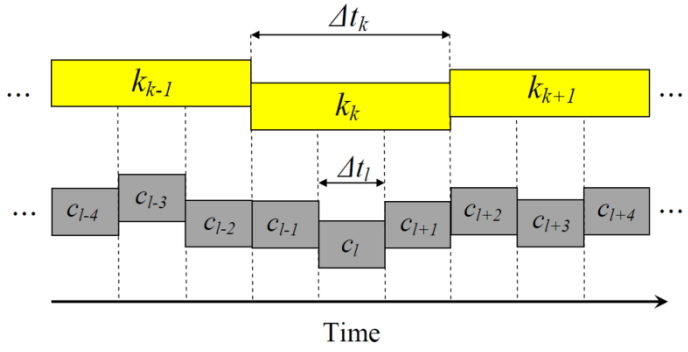

Figure 1. Time variation of the fitted parameters for p=3

Without loss of generality, one of the two unknowns can be assumed to have a faster dynamics than the other and changes over smaller time steps over Δt_k:

$$\begin{aligned}&\Delta k(t) = \Delta k_k, (k-1)\Delta t_k \le t \le k\Delta t_k, k = 1,...,m'\\ &\Delta c(t) = \Delta c_l,\ (l-1)\Delta t_l \le t \le l\Delta t_l,\ \ l = 1,...,n'\\ &\Delta t_k = p\Delta t_l, p > 1\end{aligned} \tag{10}$$

where m' and n' are the number of intervals over which the piecewise time-varying functions, $\Delta c(t)$ and $\Delta k(t)$ are defined. Further, Δt_k and Δt_l are user-selected intervals over which piecewise constant behaviour is reasonable. For ease of fitting, p is assumed to be an integer value greater than one. In this way, p values of Δc_l are fitted alongside every single value of Δk_k, as shown in Figure 1 for the case of p=3.

Identification of the unknown parameters, Δk_k and Δc_l, requires a set of linear equations, each in the form of Equation (8). For the example of Figure 1, three values of Δt_l could be chosen in each time interval Δt_l. This choice will give nine equations for each time interval Δt_k with four unknowns:

$$\mathbf{A_k}.\{x\}_k = \{I\}_k \tag{11}$$

where

$$\mathbf{A_k} = \begin{bmatrix} \phi_{1,i} & \phi_{2,i} & 0 & 0 \\ \phi_{1,i-1} & \phi_{2,i-1} & 0 & 0 \\ \phi_{1,i-2} & \phi_{2,i-2} & 0 & 0 \\ \phi_{1,i-3} & 0 & \phi_{2,i-3} & 0 \\ \phi_{1,i-4} & 0 & \phi_{2,i-4} & 0 \\ \phi_{1,i-5} & 0 & \phi_{2,i-5} & 0 \\ \phi_{1,i-6} & 0 & 0 & \phi_{2,i-6} \\ \phi_{1,i-7} & 0 & 0 & \phi_{2,i-7} \\ \phi_{1,i-8} & 0 & 0 & \phi_{2,i-8} \end{bmatrix}, \begin{matrix} k = 1,...,m' \\ i = 9,10,...,9m' \end{matrix} \tag{12}$$

$$\{x\}_k = \begin{Bmatrix} k_k \\ c_l \\ c_{l-1} \\ c_{l-2} \end{Bmatrix}, \begin{matrix} k = 1,...,m' \\ l = 3,4,...,3m' \end{matrix} \tag{13}$$

$$\{I\}_k = \begin{Bmatrix} I_i \\ I_{i-1} \\ I_{i-2} \\ I_{i-3} \\ I_{i-4} \\ I_{i-5} \\ I_{i-6} \\ I_{i-7} \\ I_{i-8} \end{Bmatrix}, \begin{matrix} k = 1,...,m' \\ i = 9,10,...,9m' \end{matrix} \tag{14}.$$

Further, $I_i, i = 1,...,9m'$ and $\phi_{1-2,i}, i = 1,...,9m'$ are defined from Equations (6) and (9) at each time step $\Delta t_i, i = 1,...,9m'$, respectively. The least squares solution of the matrix Equation (11) yields the unknown vector $\{x\}_k$.

5 SIMULATED PROOF-OF-CONCEPT STRUCTURE

To evaluate the performance of the developed real-time fault detection and diagnosis algorithm for structural health monitoring of nonlinear hysteretic base-isolation systems, a realistic base-isolated system with m=156×10^3 kg, c=2×10^4 N.s/m, k=6×10^6 N/m, α=0.6, Y=0.6 m, A=1, β=0.1, γ=0.5, and n=3 as in (Ikhouane et al. 2005; Vidal et al. 2010) is used. The simulated structure is subjected to the Loma Prieta earthquake with peak ground acceleration (PGA) of 0.27 g, and κ_1=500, κ_2=1, and κ_3=50 are used for the scaling factors.

Nonlinear dynamic analysis is performed in MATLAB® to represent the nonlinear hysteretic behaviour of the system, and the simulated responses from MATLAB® are used to provide proof of concept for the fault detection and diagnosis algorithm developed.

Moreover, the simulated system is subjected to three different worst case sudden fault patterns

including stiffness, damping, and combined stiffness and damping faults to evaluate the proposed SHM algorithm's performance in fault detection and diagnosis. Further, to assess the efficacy of the method under harmonic motions, which may be the case in marine structures, the proof-of-concept structures is subjected to a sinusoidal excitation of amplitude 0.2 g and frequency of 1 Hz. This frequency is chosen to match the natural frequency of the simulated structure and cause instability in the base-isolation system. Simulation-derived data is recorded at 1 kHz, and results are smoothened in real-time using a low-pass filter.

6 RESULTS AND DISCUSSION

Figure 2a shows a sample stiffness fault pattern and the resultant residual signal when the simulated structure is subjected to the Loma Prieta earthquake. Figures 3a and 4a show the same results for damping, and combined stiffness and damping fault examples, respectively. Finally, Figure 5a shows the calculated residual signal for a combined case of fault where the structure is under harmonic excitation.

As the figures show, the residual signal designed is well sensitive to changes as small as ±5% in stiffness and damping of the system, and the residual signal immediately goes back to its zero prior-to-fault state once the fault disappears. In some special cases, the two types of stiffness and damping faults may have equal effects on the system responses but in opposite directions. In such situations, although there is a fault in the system, the residual signal remains zero. This is expected given that the residual signal relies on the change in the system responses.

Figures 2b to 5b show the identified changes in stiffness and damping of the simulated base-isolation system using the developed diagnostic approach for each of the different fault patterns used in the simulations. These figures clearly show that the algorithm is very capable of tracking different combinations of faults in real-time.

The total computation time for each time step in the simulation is ~5e-5 s which is ~5% of the 0.001-s time step (1 kHz sampling rate) used. Moreover, the proposed algorithm only relies on the prior time step values. Therefore, the proposed algorithm is computationally quite light, and can be readily implemented as an online fault detection and diagnosis method.

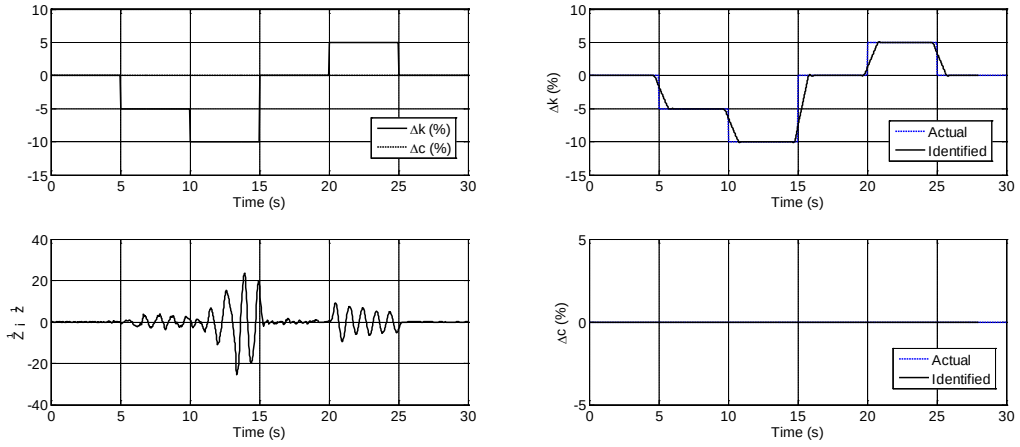

(a) (b)

Figure 2. a) Residual signal and b) identified faults for a sample stiffness fault in the simulated base-isolation system under the Loma Prieta earthquake

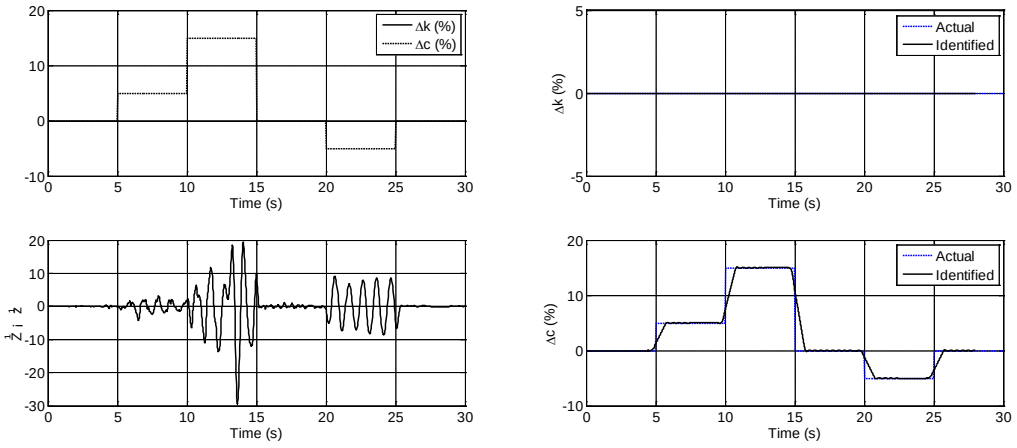

(a) (b)

Figure 3. a) Residual signal and b) identified faults for a sample damping fault in the simulated base-isolation system under the Loma Prieta earthquake

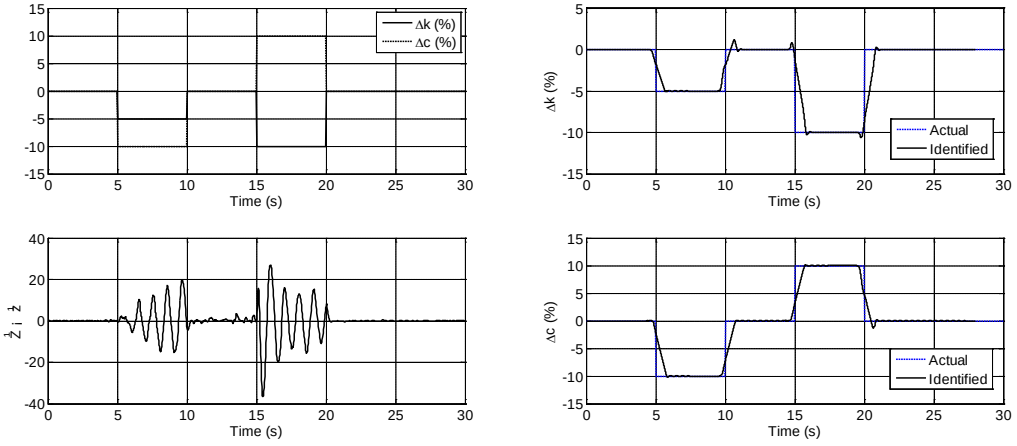

(a) (b)

Figure 4. a) Residual signal and b) identified faults for a sample combined stiffness and damping fault in the simulated base-isolation system under the Loma Prieta earthquake

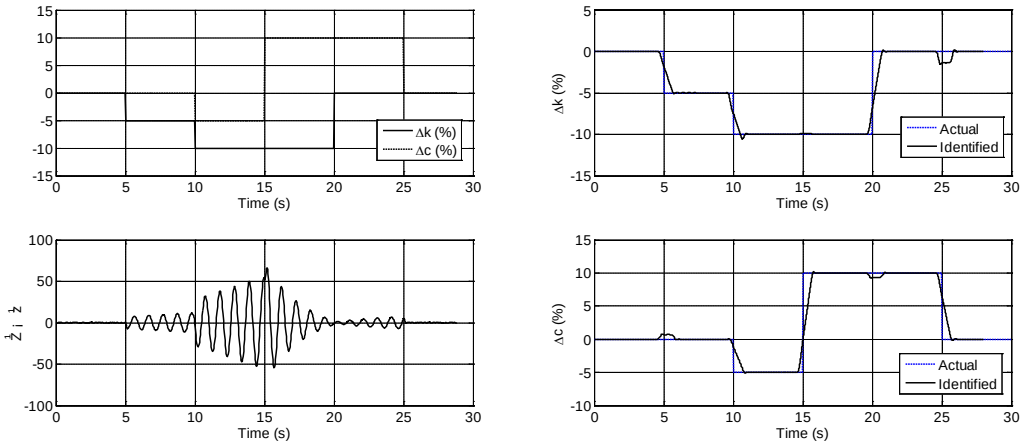

(a) (b)

Figure 5. a) Residual signal and b) identified faults for a sample combined stiffness and damping fault in the simulated base-isolation system under a harmonic ground motion of amplitude 0.2 g and frequency of 1 Hz

7 CONCLUSION

This research developed a real-time fault detection and diagnosis method for SHM of nonlinear hysteretic base-isolation systems using a simple comparison between the internal dynamics of the system with the healthy baseline model dynamics. The designed residual signal was then used for determining the type and quantifying the severity of faults occurred using least squares fitting technique. Proof-of-concept simulation results showed that for the simulated base-isolation system and the four abrupt fault scenarios considered, the developed SHM method is well capable of tracking sudden changes in stiffness and damping of the base-isolation system in real-time. The SHM method presented offers significant potential benefit in assessing base-isolation systems' safety after a major event and can provide required information by structural control methods for damage control and mitigation purposes. The method remains to be experimentally proven and further tested against noise-contaminated measurements, but is definitely a first step ahead.

REFERENCES:

Besançon, G. (2003). "High-gain observation with disturbance attenuation and application to robust fault detection." Automatica **39**(6): 1095-1102.

Bouc, R. (1967). Forced vibration of mechanical systems with hysteresis. The 14th Conference on Non-Linear Oscillation., Prague, Czechoslovakia.

Constantinou, M. and I. Tadjbakhsh (1985). "Hysteretic dampers in base isolation: random approach." Journal of Structural Engineering, ASCE **111**(4): 705-721.

Duan, G. R. and R. J. Patton (1998). Robust fault detection in linear systems using Luenberger observers. Control '98. UKACC International Conference on (Conf. Publ. No. 455).

Edwards, C., S. K. Spurgeon and R. J. Patton (2000). "Sliding mode observers for fault detection and isolation." Automatica **36**(4): 541-553.

Ikhouane, F., V. Mañosa and J. Rodellar (2005). "Adaptive control of a hysteretic structural system." Automatica **41**(2): 225-231.

Ismail, M., F. Ikhouane and J. Rodellar (2009). "The hysteresis Bouc-Wen model, a survey." Archives of Computational Methods in Engineering **16**(2): 161-188.

Kinnaert, M. (1999). "Robust fault detection based on observers for bilinear systems." Automatica **35**(11): 1829-1842.

Liberatore, S., J. L. Speyer and A. Chunliang Hsu (2006). "Application of a fault detection filter to structural health monitoring." Automatica **42**(7): 1199-1209.

Mhaskar, P., C. McFall, A. Gani, P. D. Christofides and J. F. Davis (2008). "Isolation and handling of actuator faults in nonlinear systems." Automatica **44**(1): 53-62.

Patton, R. J. (1997). "Robustness in model-based fault diagnosis: The 1995 situation." Annual Reviews in Control **21**: 103-123.

Saif, M. (2002). Fault diagnosis based on equivalent control concept. Automation Congress, 2002 Proceedings of the 5th Biannual World.

Spencer, J. B. F. and S. Nagarajaiah (2003). "State of the Art of Structural Control." Journal of Structural Engineering **129**(7): 845-856.

Vidal, Y., L. Acho, F. Pozo and J. Rodellar (2010). Fault detection in base-isolation systems via a restoring force observer. 2010 Conference on Control and Fault Tolerant Systems. Nice, France, IEEE**:** 777-782.

Wen, Y.-K. (1976). "Method for random vibration of hysteretic systems." Journal of Engineering Mechanics Division, ASCE **102**(2): 249-263.